Optical Coherence Tomography Angiography Macular and Peripapillary Vessel Perfusion Density in Healthy Subjects, Glaucoma Suspects, and Glaucoma Patients

Giacinto Triolo,[1] Alessandro Rabiolo,[1] Nathan D. Shemonski,[2] Ali Fard,[2] Federico Di Matteo,[1] Riccardo Sacconi,[1] Paolo Bettin,[1] Stephanie Magazzeni,[2] Giuseppe Querques,[1] Luis E. Vazquez,[3] Piero Barboni,[1] and Francesco Bandello[1]

[1]Department of Ophthalmology, University Vita-Salute, San Raffaele Scientific Institute, Milan, Italy
[2]Carl Zeiss Meditec, Inc., Dublin, California, United States
[3]Bascom Palmer Eye Institute, University of Miami Miller School of Medicine, Miami, Florida, United States

Correspondence: Giacinto Triolo, Department of Ophthalmology, University Vita-Salute, San Raffaele Scientific Institute, Via Olgettina 60, 20133 Milan, Italy; triolo.giacinto@hsr.it.

Submitted: August 24, 2017
Accepted: October 4, 2017

Citation: Triolo G, Rabiolo A, Shemonski ND, et al. Optical coherence tomography angiography macular and peripapillary vessel perfusion density in healthy subjects, glaucoma suspects, and glaucoma patients. *Invest Ophthalmol Vis Sci*. 2017;58:5713–5722. DOI:10.1167/iovs.17-22865

Purpose. To evaluate macular and peripapillary vessel perfusion density (VD) in glaucoma suspects (GS) and glaucoma patients; to correlate ganglion cell–inner plexiform layer (GCIPL) and retinal nerve fiber layer (RNFL) thicknesses with macular and peripapillary VD; and to evaluate the diagnostic accuracy of the structural and vascular parameters.

Methods. A consecutive series of GS, glaucoma patients, and healthy subjects was prospectively recruited from July 1, 2016, to January 31, 2017. All subjects underwent standard automated perimetry, spectral-domain optical coherence tomography (OCT), and 6 × 6-mm optical coherence tomography angiography (OCT-A) centered on the fovea and optic nerve.

Results. Forty controls, 40 GS, and 40 glaucoma patients were enrolled. Peripapillary RNFL, GCIPL, and macular RNFL thicknesses significantly decreased in the glaucoma group compared to controls and GS ($P < 0.01$). Peripapillary VD in average and in the superior and inferior quadrants decreased in the glaucoma group ($P \leq 0.001$); conversely, macular VD was not statistically different across groups ($P > 0.05$). At the peripapillary area, a correlation between RNFL thickness and VD was found; conversely, no statistically significant correlation was found between GCIPL thicknesses and macular VD (all $P > 0.05$) in all groups. Peripapillary RNFL and GCIPL showed higher diagnostic capacity compared to peripapillary and macular VDs.

Conclusions. Structural damage is evident both in the peripapillary and in macular areas. Vascular damage seems to be less prominent, as it was seen only for the glaucoma group and at the radial peripapillary plexus. Diagnostic abilities are excellent for structural variables, less so but still good for peripapillary VD, and poor for macular VD.

Keywords: glaucoma, glaucoma suspect, optical coherence tomography, optical coherence tomography angiography, vessel perfusion density

Primary open-angle glaucoma (POAG) is a chronic, progressive optic neuropathy, whose main risk factor is an elevated intraocular pressure (IOP).[1] As previously demonstrated, it is characterized by a specific pattern of damage affecting both the retinal ganglion cells (RGCs) and their axons, meaning the retinal nerve fibers (RNFs), eventually leading to the typical corresponding visual field (VF) defects.[1] The glaucomatous damage is believed to involve the peripapillary RNFs primarily; however, some authors have shown that a macular involvement is also detectable in an early stage of the disease.[2] Although the pathogenesis of glaucoma is not fully understood, interest in the vascular component has recently increased.

Optical coherence tomography angiography (OCT-A) has been recently introduced as a noninvasive and reproducible tool to provide a qualitative and quantitative evaluation of the microvasculature of different retinal layers.[3] For these reasons OCT-A has been used to evaluate the peripapillary vessel density in healthy subjects and glaucoma patients, showing that capillary dropout occurs in the peripapillary area in patients with retinal nerve fiber layer (RNFL) and VF defects.[4–9] Further, even though the macular involvement in glaucoma has been demonstrated, few papers have focused on the macular microvasculature in patients affected by this disease.[10–15]

The purposes of the present study were (1) to evaluate both macular and peripapillary vessel perfusion density (VD) in glaucoma suspects (GS) and glaucoma (G) patients, (2) to correlate macular RGC and RNFL defects with macular and peripapillary VD, and (3) to evaluate the diagnostic accuracy of RGC and RNFL thicknesses and vascular parameters in detecting glaucoma.

Methods

Study Participants

A consecutive series of GS and glaucoma patients was prospectively recruited from July 1, 2016, to January 31, 2017,

in the present study conducted at the Department of Ophthalmology, San Raffaele Scientific Institute, Milan, Italy. All participants provided written informed consent to participate in observational studies. The study received institutional review board approval from the ethics committee of San Raffaele Hospital, and adhered to the tenets of the Declaration of Helsinki. Data from the patients enrolled were compared to a cohort of age- and sex-matched healthy subjects.

All study participants underwent a complete ophthalmologic examination, including best-corrected visual acuity (BCVA) measurement, slit-lamp biomicroscopy, IOP measurement with Goldmann applanation tonometry, gonioscopy, ultrasound pachymetry, and dilated fundus examination. Participants also completed standard automated perimetry (SAP) (30-2 Swedish Interactive Threshold Algorithm; Humphrey Field Analyzer II; Carl Zeiss Meditec, Inc., Dublin, CA, USA), spectral-domain optical coherence tomography (OCT) (Cirrus HD-OCT 5000; Carl Zeiss Meditec, Inc.), and swept-source OCT-A (PLEX Elite 9000; Carl Zeiss Meditec, Inc.). Only participants with high-quality HD-OCT and OCT-A scans and at least two reliable SAP tests were included in this study.

Common inclusion criteria for all groups were age $\geq$ 18 years, an open iridocorneal angle on gonioscopy, BCVA $\geq$ 20/40, and a refractive error between -3 and $+3$ diopters. Common exclusion criteria for all groups were presence of any other retinal or optic nerve disease; previous surgery other than uneventful cataract surgery $\geq$ 6 months prior enrollment; inability to fixate; incapacity to release informed consent; significant media opacity preventing adequate image quality; refractive error < -3 or $> +3$ diopters.

Inclusion criteria for GS were (1) a minimum of two reliable normal VFs, defined as a pattern standard deviation (PSD) within 95% confidence limits and a glaucoma hemifield test (GHT) result within normal limits; (2) average and quadrant RNFL thickness within 95% and 99% confidence limits, respectively; (3) vertical cup-to-disc ratio (VCDR) $\geq$ 0.5 (based on HD-OCT measurements); (4) VCDR asymmetry $\geq$ 0.2, with the minor VCDR $\geq$ 0.4; (5) IOP $\leq$ 21 mm Hg in three consecutive visits without any treatment. The GS were enrolled in the study if they met criteria 1 and 2, and at least one among criteria 3, 4, and 5.

Inclusion criteria for patients with glaucoma were the following: (1) repeatable glaucomatous VF damage defined as a GHT result outside normal limits and a PSD outside 95% normal limits; (2) glaucomatous VF abnormalities defined by a cluster of $\geq$ 3 adjacent points in the pattern deviation (PD) plot with a probability of $<$5% including at least 1 point having a probability $<$1% in at least two repeatable and consecutive SAP tests.

Healthy subjects were required to have (1) an IOP $\leq$ 21 mm Hg with no history of elevated IOP; (2) normal-appearing optic disc and intact neuroretinal rim on clinical examination; (3) average and quadrant RNFL thickness within 99% confidence limits; and (4) a minimum of two reliable normal VFs, defined as a PSD within 95% confidence limits and a GHT result within normal limits.

Spectral-Domain Optical Coherence Tomography Imaging

Peripapillary (Optic Disc 200×200 Cube protocol) and macular scans (Macular 512×128 Cube protocol) were acquired using Cirrus 5000 HD-OCT (Carl Zeiss Meditec, Inc.) for RNFL and ganglion cell–inner plexiform layer (GCIPL) thickness measurements.

The manufacturer's released software was used to calculate RNFL and GCIPL thicknesses, as previously described.[16,17] Poor-quality images showing eye motion, blinking artifacts, poor centration, and signal strength $<$ 7 were excluded from the analysis. Average (Avg), superior (S), nasal (N), inferior (I), and temporal (T) peripapillary RNFL (pRNFL) thickness values, as well as average (Avg), superotemporal (ST), S, superonasal (SN), inferonasal (IN), I, and inferotemporal (IT) macular GCIPL and RNFL (mRNFL) thickness values, were recorded and included in the analysis.

The GCIPL thickness was calculated from the outer boundary of the RNFL and the outer boundary of the IPL. The difference between the RNFL and the IPL outer boundary segmentations yields the combined thickness of the GCL and the IPL. Although it might be ideal to measure the GCL and IPL individually, the boundary between these two layers is anatomically indistinct so that they are difficult to robustly distinguish from each other. Nonetheless, the combined thickness is considered to be indicative of the health of RGCs.[16,17]

OCT-Angiography (OCT-A) Imaging

Peripapillary and macular 6 × 6-mm OCT-A scans centered on the optic nerve head (ONH) and the fovea, respectively, were acquired by using the PLEX Elite 9000 device (Carl Zeiss Meditec, Inc.). A fully automated retinal layer segmentation algorithm was applied to three-dimensional structural OCT data in order to segment the inner limiting membrane (ILM) and the outer boundary of the inner plexiform layer (IPL) for macular scans as well as the outer boundary of RNFL for peripapillary scans. The segmentation results were then applied to OCT-A flow intensity data to obtain vascular images. Maximum projection analyses of the flow intensity were performed to generate the superficial retinal vascular plexus from ILM to IPL for macular scans and the radial peripapillary capillary (RPC) plexus from ILM to RNFL for peripapillary scans. Note that only the retinal superficial vascular plexus and the RPC plexus were analyzed in this study.

All raw data were exported and sent to Carl Zeiss Meditec, Inc. Ophthalmic Diagnostics R&D, which analyzed the data with a prototype algorithm and provided the VD values.

The peripapillary scans were postprocessed as shown in Figures 1A, 1B, and 1C: a ring-shaped region of interest (ROI) centered on the ONH (inner circle 2-mm diameter, outer circle 6-mm diameter) was overimposed onto the peripapillary OCT-A scan (Figs. 1A, 1B). The areas outside of the outer circle and within the inner circle (including the ONH) were colored out black and were excluded from the analysis (Fig. 1C); thus, only the parts of the image included in the ROI were used to calculate the RPC-VD. Finally, the large vessels were excluded from the image in order to calculate only the capillary density. Avg, S, N, I, and T RPC-VDs were calculated.

The macular scans were postprocessed as shown in Figures 1D, 1E, and 1F: A ROI equal in size and shape to the one used in the macular GCIPL thickness analysis incorporated in the Cirrus device was overimposed on the macular OCT-A scan (Figs. 1D, 1E). The areas outside of the outer circle and within the inner circle (including the foveal avascular zone, FAZ) were colored out black and were excluded from the analysis (Fig. 1F); therefore, only the parts of the image included in the ROI were used to calculate the macular superficial retinal capillary vessel perfusion density (SRC-VD). Vessel perfusion density was defined as the total area of perfused vasculature per unit area. It was calculated by segmenting blood vessel/capillaries in the en face OCT-A images and subsequently calculating the total area identified as vessel divided by the total area of a ROI. Note that in order to calculate capillary perfusion density for peripapillary scans, large retinal vessels were identified and excluded from the calculations. Avg, ST, S, SN, IN, I, and IT SRC-VD were reported.

Investigative Ophthalmology & Visual Science

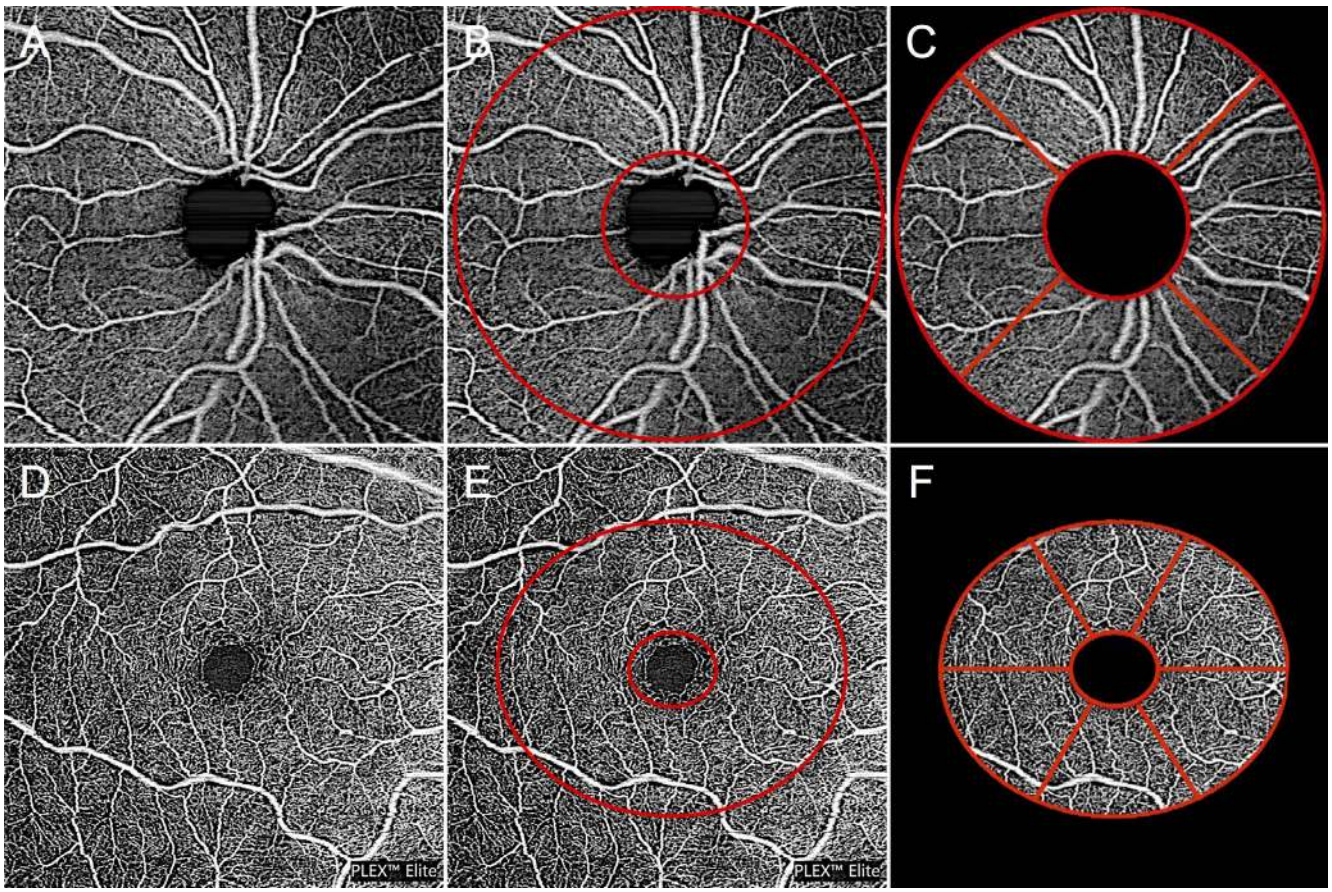

FIGURE 1. (**A–C**) Postprocessing of the peripapillary OCT-A images. (**A**) En face image centered on the optic nerve head (ONH), showing the semiautomated segmentation of the radial peripapillary capillaries (RPC). The deeper retinal layers are not included in the analysis. (**B**) A ring-shaped region of interest (ROI) consisting of two circles (inner circle 2-mm diameter, outer circle 6-mm diameter) was overimposed onto the peripapillary OCT-A scan. (**C**) The areas outside of the outer circle and within the inner circle (including the ONH) were colored out black, and were excluded from the analysis. Therefore, only the parts of (**A**) included in the ROI were used to calculate the RPC vessel perfusion density (RPC-VD). Furthermore, the ROI was divided into superior, nasal, inferior, and temporal quadrants, according to the RNFL thickness analysis of the Cirrus OCT. Finally, large vessels were excluded from the image in order to calculate only the capillary density (not shown in the photo). (**D–F**) Postprocessing of the macular OCT-A images. (**D**) En face image centered on the fovea, showing the semiautomated segmentation of the superficial retinal capillaries (SRC). (**E**) A ROI equal in size and shape to the one used in the macular GCIPL thickness analysis incorporated in the Cirrus OCT was overimposed onto the macular OCT-A scan. (**F**) The areas outside of the outer circle and within the inner circle (including the foveal avascular zone, FAZ) were colored out black and were excluded from the analysis. Thus, only the parts of (**D**) included in the ROI were used to calculate the macular SRC vessel perfusion density (SRC-VD). The ROI was then divided into six sectors (superotemporal, superior, superonasal, inferonasal, inferior, inferotemporal), according to the GCIPL thickness analysis of the Cirrus OCT.

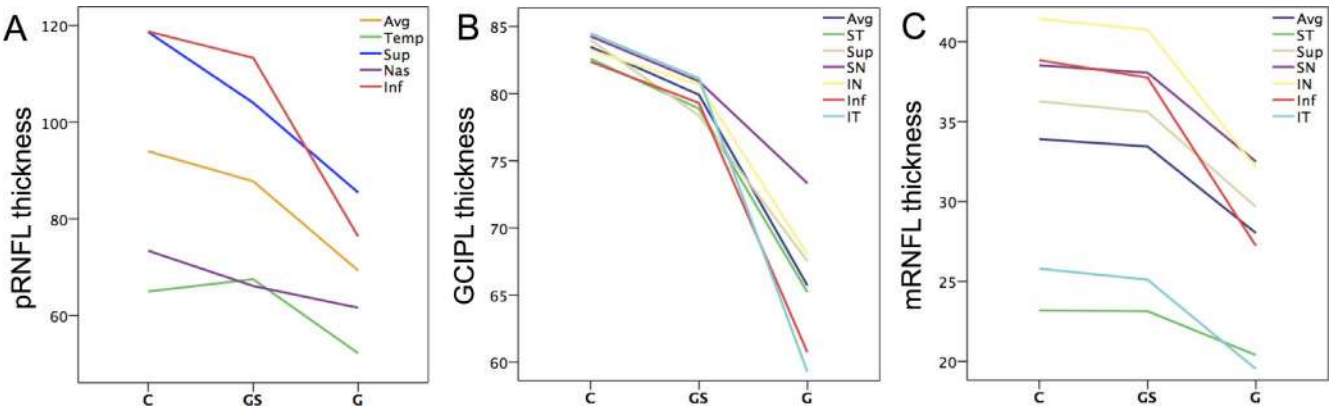

FIGURE 2. Mean average and sectorial thicknesses (mm) of peripapillary RNFL (pRNFL), GCIPL, and macular RNFL (mRNFL) (**A–C**, respectively) in controls (C), glaucoma suspects (GS), and glaucoma (G) patients. All parameters were significantly thinner among groups (ANOVA $P < 0.001$; data shown in Table 2).

Investigative Ophthalmology & Visual Science

Table 1. Demographics and Clinical Characteristics of the Study Cohort. All Parameters, Except for Sex, Are Shown as Mean ± SD

	C	GS	G	ANOVA
N	40	40	40	
Age	60.9 ± 17.3	61.7 ± 16.6	63.6 ± 11.7	0.38
Sex, male %	51.3	55.5	49.5	0.23
RE	−0.07 ± 0.18	0.11 ± 0.32	−0.05 ± 0.21	0.31
IOP, mm Hg	15.3 ± 2.10	15.5 ± 3.11	14.8 ± 1.17	0.09
VCDR	0.30 ± 0.09	0.58 ± 0.15	0.71 ± 0.10	<0.01
Disc area, mm^2	1.91 ± 0.26	1.93 ± 0.48	1.82 ± 0.46	0.35
VF MD	−0.71 ± 1.36	−1.57 ± 1.77	−5.45 ± 2.27	<0.001

RE, refractive error.

Statistical Analysis

Assuming that healthy subjects have a RPC-VD of 20.5 ± 2.3%,[6] 33 individuals for each group could permit highlighting a difference of at least 10% of RPC-VD with a power of 90% and an α error of 5%. We decided to enroll 40 subjects in each group in order to account for differences in study populations, instrumentation, postprocessing algorithms, or patients to exclude (e.g., poor image quality, artifacts).

One eye per patient was selected for the analysis. In the control group, the eye was randomly selected. In the GS and G groups, the affected eye was selected; if both eyes met the inclusion criteria, only one eye was randomly selected.

Continuous variables are described as means ± standard deviation (SD). All variables followed a normal distribution using the D'Agostino-Pearson test. Significant differences between GCIPL, mRNFL, pRNFL, RPC-VD, and SRC-VD parameters across groups were tested with 1-way analysis of variance (ANOVA), and Bonferroni test was used for post hoc analysis. The correlation between different parameters was tested with 2-tailed Pearson's correlation analysis.

Area under the receiver operating characteristic curves (AUROCs) was used to test the diagnostic accuracy of several parameters to detect glaucoma. Statistical analyses were performed using commercially available statistical software (SPSS version 17.0; SPSS, Inc., Chicago, IL, USA). Statistical significance was defined at $P < 0.05$.

Results

Forty controls, 40 GS, and 40 G patients were enrolled in the study. All groups' demographics are summarized in Table 1. The three groups were matched for age and sex (ANOVA $P > 0.05$). Vertical cup-to-disc ratio and visual field mean deviation (VF MD) were statistically greater and lower, respectively, in the G group compared to the C and GS groups (ANOVA, $P < 0.01$ and $P < 0.001$, respectively).

HD-OCT Parameters

Peripapillary RNFL, GCIPL, and macular RNFL (mRNFL) average and sectorial thicknesses (mean ± SD, μm) in the three groups are shown in Table 2 and Figure 2. All pRNFL, GCIPL, and mRNFL thicknesses were significantly decreased in the G group compared to the C and GS groups (ANOVA, all $P < 0.01$), except for the ST mRNFL thickness, which was not statistically different between groups (ANOVA, $P = 0.077$). The Bonferroni post hoc analysis revealed thinner Avg, S, and N pRNFL thicknesses in the GS compared to the C group. However, no differences were found in all GCIPL and mRNFL thicknesses between C and GS.

Plex Elite 9000 OCT-A Parameters

Radial peripapillary capillary vessel perfusion density (RPC-VD) and SRC-VD parameters (mean ± SD) in C, GS, and G are listed in Table 3. On the one hand, Avg and all quadrants' RPC-VD parameters were decreased among groups (ANOVA, all $P < 0.01$), with the exception of the nasal sector (ANOVA, $P = 0.219$). On the other hand, Avg and all sectorial SRC-VD parameters were not statistically different across groups (ANOVA, $P > 0.05$). As shown in Figures 3A, 3B, and 3C, S,

Table 2. Peripapillary RNFL (pRNFL), GCIPL, and Macular RNFL (mRNFL) Thickness (Mean ± SD, μm) in Controls, Glaucoma Suspects, and Glaucoma; ANOVA and Bonferroni Post Hoc Analysis Show the Statistical Differences Across Groups and Between C and GS, Respectively

	C	GS	G	Bonferroni C vs. GS	ANOVA
pRNFL					
Sup	118.67 ± 13.99	104.03 ± 19.36	85.44 ± 26.79	**0.009**	**<0.001**
Nas	73.41 ± 8.33	66.11 ± 11.49	61.60 ± 11.51	**0.010**	**<0.001**
Inf	118.77 ± 15.54	113.33 ± 15.82	76.35 ± 16.63	>0.05	**<0.001**
Temp	64.97 ± 11.42	67.50 ± 11.78	52.19 ± 12.10	>0.05	**<0.001**
Avg	23.97 ± 8.92	87.78 ± 9.96	69.30 ± 11.21	**0.028**	**<0.001**
GCIPL					
ST	82.59 ± 7.12	78.89 ± 7.81	65.20 ± 14.50	>0.05	**<0.001**
Sup	84.00 ± 8.80	78.36 ± 10.74	67.53 ± 13.82	>0.05	**<0.001**
SN	84.27 ± 8.52	80.92 ± 8.11	73.33 ± 12.42	>0.05	**<0.001**
IN	83.24 ± 7.63	80.67 ± 7.50	68.03 ± 12.63	>0.05	**<0.001**
Inf	82.37 ± 7.10	79.31 ± 6.51	60.73 ± 12.84	>0.05	**<0.001**
IT	84.49 ± 8.15	81.14 ± 6.06	59.28 ± 16.27	>0.05	**<0.001**
Avg	83.49 ± 7.33	79.92 ± 6.36	65.70 ± 10.88	>0.05	**<0.001**
mRNFL					
ST	23.19 ± 2.20	23.14 ± 3.40	20.40 ± 7.48	>0.05	0.077
Sup	36.26 ± 4.27	35.61 ± 6.78	29.67 ± 8.45	>0.05	**0.001**
SN	38.52 ± 5.03	38.06 ± 6.79	32.50 ± 8.25	>0.05	**0.002**
IN	41.42 ± 4.86	40.75 ± 7.06	32.13 ± 8.83	>0.05	**<0.001**
Inf	38.84 ± 3.93	37.75 ± 4.19	27.23 ± 8.47	>0.05	**<0.001**
IT	25.81 ± 2.39	25.11 ± 2.78	19.53 ± 8.86	>0.05	**<0.001**
Avg	33.90 ± 3.09	33.44 ± 4.23	28.03 ± 8.35	>0.05	**<0.001**

Bold values indicate statistical significance. Sup, superior; Nas, nasal; Inf, inferior; Temp, temporal.

Table 3. Radial Peripapillary Capillary Vessel Density (RPC-VD) and Superficial Retinal Capillary Vessel Density (SRC-VD) (Mean ± SD) in Controls, Glaucoma Suspects, and Glaucoma; ANOVA Shows the Statistical Differences Among Groups

	C	GS	G	ANOVA
RPC-VD				
Sup	0.509 ± 0.02	0.510 ± 0.03	0.479 ± 0.04	**<0.001**
Nas	0.519 ± 0.10	0.539 ± 0.02	0.510 ± 0.03	0.219
Inf	0.525 ± 0.02	0.525 ± 0.02	0.475 ± 0.05	**<0.001**
Temp	0.561 ± 0.02	0.564 ± 0.02	0.546 ± 0.03	**<0.01**
Avg	0.534 ± 0.01	0.536 ± 0.02	0.504 ± 0.03	**<0.001**
SRC-VD				
ST	0.450 ± 0.03	0.443 ± 0.06	0.419 ± 0.07	0.089
Sup	0.450 ± 0.03	0.440 ± 0.06	0.420 ± 0.09	0.167
SN	0.462 ± 0.02	0.446 ± 0.04	0.436 ± 0.07	0.104
IN	0.465 ± 0.02	0.449 ± 0.04	0.454 ± 0.05	0.251
Inf	0.459 ± 0.03	0.439 ± 0.05	0.446 ± 0.08	0.427
IT	0.454 ± 0.03	0.428 ± 0.07	0.440 ± 0.06	0.178
Avg	0.458 ± 0.02	0.441 ± 0.05	0.437 ± 0.05	0.125

Bold values indicate statistical significance. Sup, superior; Nas, nasal; Inf, inferior; Temp, temporal.

I, and Avg RPC-VD were decreased in the G group compared to both C and GS (ANOVA, Bonferroni post hoc analysis, all $P \leq 0.001$); no differences in these parameters were found between the C and GS groups. Conversely, Avg SRL-VD was not decreased across groups, nor between pairs of groups (Fig. 3D). None of the OCT-A parameters correlated significantly with spherical equivalent ($P > 0.05$).

Correlation Between OCT and OCT-A Parameters

Table 4 shows the Pearson's correlation coefficients between pRNFL/GCIPL thicknesses and the corresponding RPC-VD/SRC-VD parameters across the three groups. In the C group, only the N and T quadrants showed a borderline significant correlation between pRNFL and RPC-VD ($P < 0.05$), while in the GS group, I and Avg showed a stronger correlation ($P < 0.05$ and $P \leq 0.01$, respectively). Further, in the G group, a strong correlation was found between S, I, and Avg pRNFL thickness and RPC-VD parameters (all $P < 0.001$). The increasing correlation trend between Avg pRNFL and Avg RPC-VD among the three groups is also displayed in Figure 4.

Conversely, no statistically significant correlation was found between GCIPL thicknesses and SRC-VD parameters (all $P > 0.05$) in all groups, except for a borderline significant correlation between Avg GCIPL and Avg SRC-VD in the G group. Finally, no significant correlation was found between mRNFL thicknesses and SRC-VD parameters (data not shown).

Correlation Between OCT-A Parameters and VF MD

Table 4 also reports the Pearson's correlation coefficients between RPC-VD/SRC-VD parameters and VF MD. On the one hand, no significant correlation was found between any of

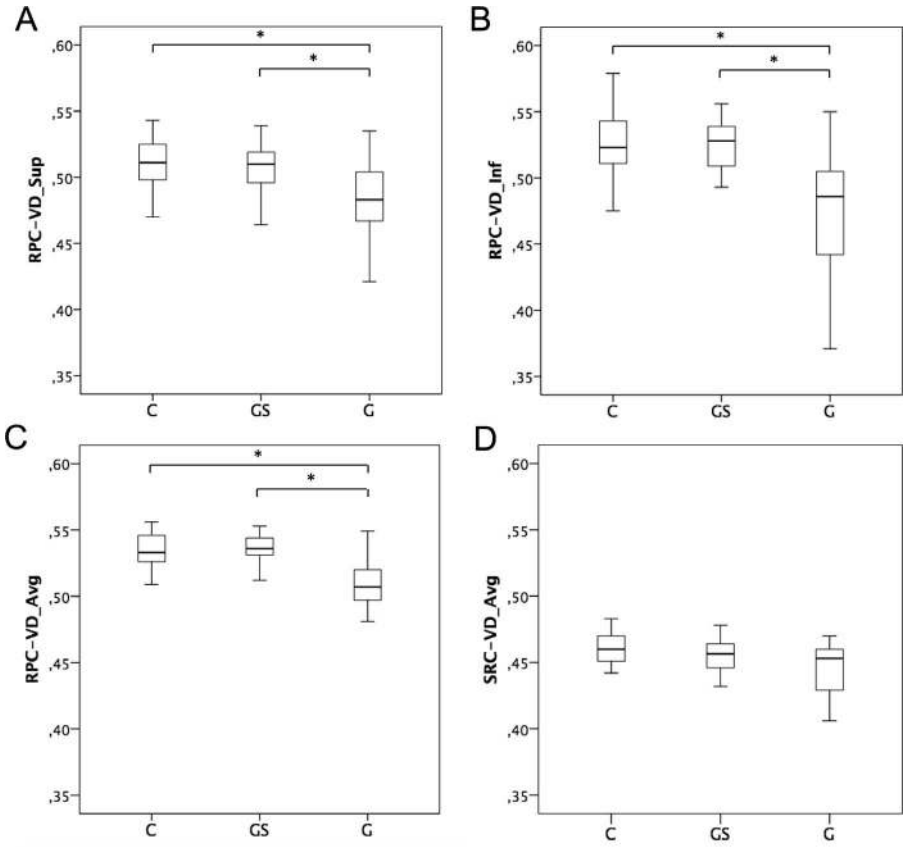

Figure 3. Box plots showing the superior (Sup), inferior (Inf), and average (Avg) radial peripapillary capillary vessel perfusion density (RPC-VD) (**A**–**C**, respectively) and average (Avg) superficial retinal capillary vessel perfusion density (SRC-VD) (**D**) in controls (C), glaucoma suspects (GS), and glaucoma (G) patients. The *boxes* show the 75th percentile (*top line*), the median (*middle line*), and the 25th percentile (*bottom line*). The *whiskers* show the maximum (*top bar*) and minimum (*bottom bar*) values. *Asterisks* show the statistical difference between pairs of groups. *$P \leq 0.001$.

Table 4. Pearson's Correlation Coefficients Between RPC-VD Parameters and the Corresponding Sectorial pRNFL Thicknesses, and Between SRC-VD Parameters and the Corresponding Sectorial GCIPL Thicknesses

	C	GS	G	G VF MD
pRNFL				
RPC-VD				
Sup	−0.245	0.331	0.616‡	0.567†
Nas	0.433*	0.389	0.309	0.412
Inf	0.114	0.489*	0.546‡	0.637‡
Temp	0.520*	0.280	0.330	0.214
Avg	0.196	0.470†	0.773‡	0.675‡
GCIPL				
SRC-VD				
ST	0.022	0.051	0.194	0.147
Sup	−0.106	0.212	0.367	0.400
SN	−0.132	0.149	0.216	0.002
IN	−0.069	0.105	0.294	0.082
Inf	0.076	0.152	0.343	0.152
IT	0.249	0.104	0.352	0.172
Avg	0.043	0.242	0.395*	0.139

Data are reported for controls (C), glaucoma suspects (GS), and glaucoma (G). The correlation between RPC-/SRC-VD parameters and VF MD in the glaucoma group is also shown. Sup, superior; Nas, nasal; Inf, inferior; Temp, temporal.

* $P < 0.05$.

† $P \leq 0.01$.

‡ $P \leq 0.001$.

these parameters in the C and GS groups (data not shown). Nevertheless, this was not the case for the G group, in which a highly significant correlation was found between S, I, Avg RPC-VD, and VF MD. No correlation was found between SRC-VD parameters and VF MD.

Differences in the Diagnostic Capacity of Detecting Glaucoma Between OCT and OCT-A Parameters

Figure 5 shows the AUROCs representing the diagnostic accuracy in detecting glaucoma of average peripapillary RNFL thickness (pRNFL_Avg) versus average radial peripapillary capillary vessel perfusion density (RPC-VD_Avg), and average GCIPL thickness (GCIPL_Avg) versus average superificial retinal capillary vessel perfusion density (SRC-VD_Avg) in C versus G (Figs. 5A, 5B) and in GS versus G (Figs. 5C, 5D).

The AUROC values of pRNFL, GCIPL, mRNFL, RPC-VD, and SRC-VD parameters are listed in Table 5.

Overall, pRNFL and GCIPL showed higher diagnostic capacities in detecting glaucoma compared to RPC-VD and SRC-VD. Macular RNFL showed lower AUROC values compared to other structural parameters, such as pRNFL and GCIPL. Furthermore, while RPC-VD parameters had good AUROC values (albeit lower than pRNFL thicknesses), SRC-VD showed the lowest AUROC values among all parameters considered.

Discussion

In the present study, we compared structural OCT-derived (i.e., pRNFL, GCIPL, and mRFNL thicknesses) and vascular OCT-A–derived (i.e., RCP-VD and SRC-VD) parameters across patients with glaucoma, GS, and healthy subjects. In addition, the correlations between structural and vascular variables and their diagnostic abilities were also assessed.

Although the pure evaluation of structural OCT parameters in glaucoma lies outside the primary aim of this study, some aspects are worth being mentioned. Predictably, GCIPL, mRNFL, and pRNFL were thinner in glaucomatous eyes compared to both healthy subjects and GS. However, the most interesting findings of structural data were found when comparing C with GS. On the one hand, pRNFL parameters showed significant thinning in GS compared to C. This result agrees with what has already been demonstrated, that is, a mild pRNFL thickness reduction in GS compared to healthy eyes, preceding more pronounced RNFL and VF defects typical of glaucoma.[18–20] For this reason, pRNFL thickness is suggested to be a helpful parameter in assessing the risk of developing glaucomatous damage. On the other hand, mRNFL and GCIPL thicknesses remained unchanged in GS compared to C. While macular damage has been clearly demonstrated in early glaucoma,[2] few studies are available about GCIPL thinning in GS.[16,21,22] Our results corroborate the previous findings.

When it comes to the vascular component of glaucoma, a relationship between ocular blood flow and this disease has long been hypothesized. Chronic impairment of ocular blood flow with subsequent ischemia–reperfusion damage has been advocated as a major pathogenic factor.[23] Several instruments have been applied to inquire into ocular blood flow in glaucoma, including fluorescein and indocyanine green angiography,[24] laser speckle flowgraphy,[25] color Doppler imaging,[26] Doppler OCT,[27] confocal scanning laser Doppler flowmetry,[28] and retinal functional imager.[29] Although welcomed with great enthusiasm, none of these eventually broke

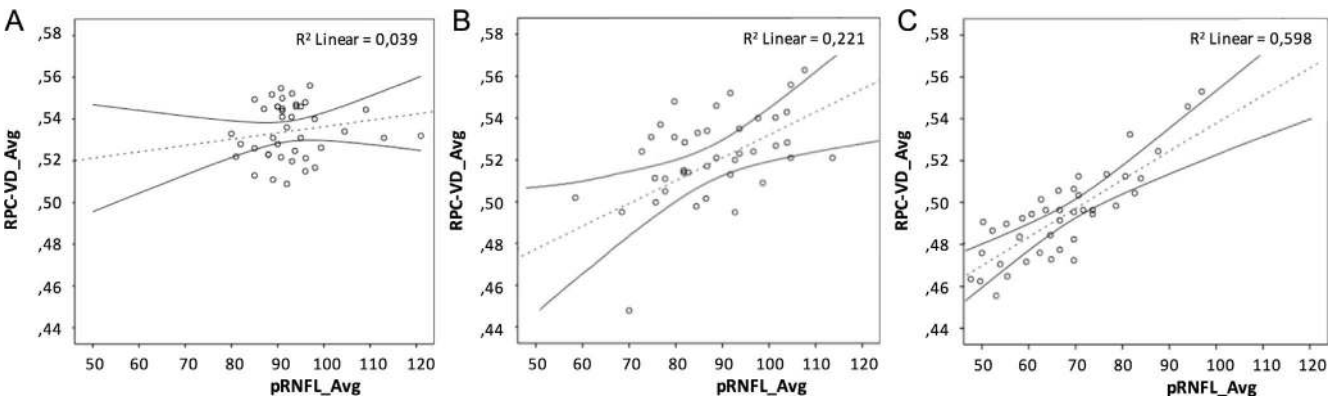

Figure 4. Correlation between average radial peripapillary capillary vessel perfusion density (RPC-VD_Avg) and average peripapillary retinal nerve fiber layer thickness (pRNFL_Avg) in controls (**A**), glaucoma suspects (**B**), and glaucoma (**C**).

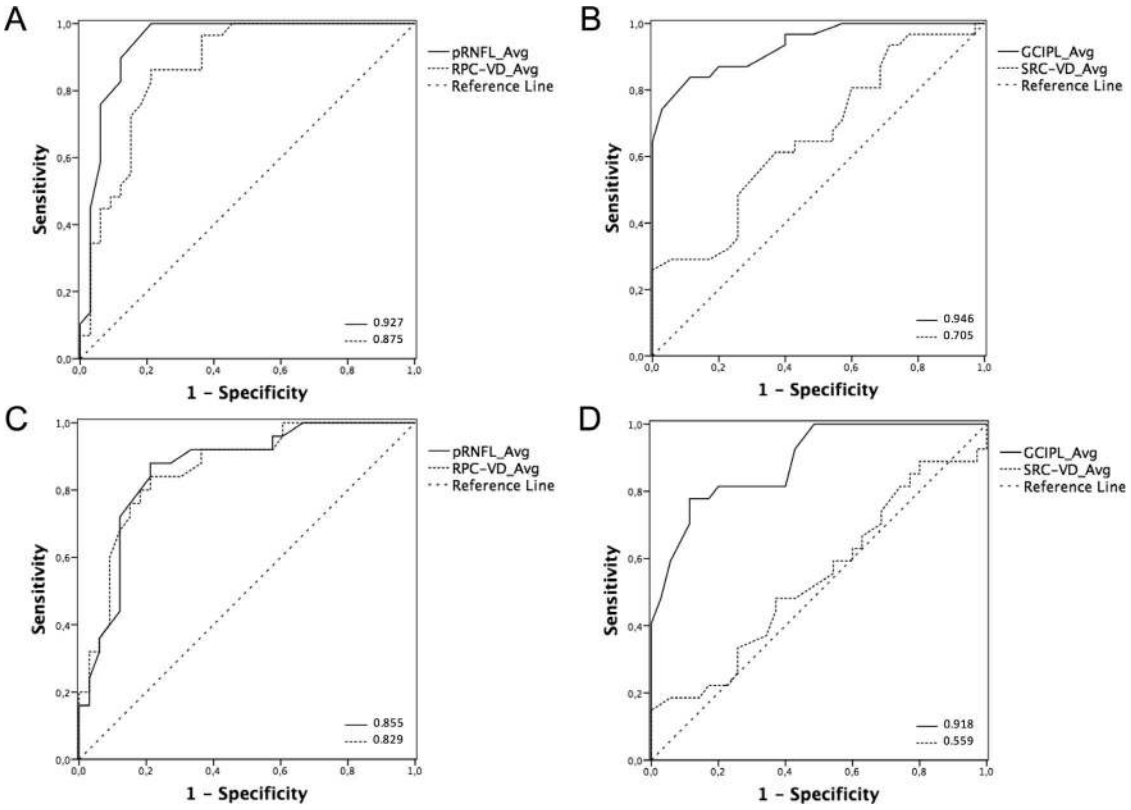

Figure 5. Area under the receiver operating characteristic curves (AUROCs) showing the diagnostic accuracy of average peripapillary RNFL thickness (pRNFL_Avg) versus average radial peripapillary capillary vessel perfusion density (RPC-VD_Avg), and average GCIPL thickness (GCIPL_Avg) versus average superificial retinal capillary vessel perfusion density (SRC-VD_Avg) in controls versus glaucoma (**A**, **B**) and in glaucoma suspects versus glaucoma (**C**, **D**). Corresponding AUROC values are also reported.

into clinical practice due to several limitations (e.g., reliability, invasiveness, accuracy, precision, need for expert staff members).[30] Recently, OCT-A was introduced in the market, and it has several advantages over previous devices since it is a dye-less, reliable, depth-resolved, user-friendly technique that enables evaluation of retinal and choroidal circulation both in the macula and in the ONH.[3] OCT-A allows study of the retinal vascular plexus separately, and therefore it permits distinguishing radial peripapillary, superficial, and deep capillary plexuses. In the present study, we focused on inner vascular plexuses

Table 5. Area Under the Receiver Operating Characteristic Curve Values of Peripapillary Retinal Nerve Fiber Layer, Ganglion Cell–Inner Plexiform Layer, Macular Retinal Nerve Fiber Layer, Radial Peripapillary Capillary Vessel Perfusion Density, and Macular Superficial Retinal Capillary Vessel Perfusion Density (SRC-VD) Parameters

	C vs. GS			GS vs. G			C vs. G		
	pRNFL	**RPC-VD**	***P* Value**	**pRNFL**	**RPC-VD**	***P* Value**	**pRNFL**	**RPC-VD**	***P* Value**
Sup	0.687	0.562	*	0.670	0.679	*	0.872	0.735	†
Nas	0.708	0.491	†	0.606	0.728	*	0.782	0.732	*
Inf	0.508	0.438	*	0.931	0.844	†	0.958	0.799	‡
Temp	0.470	0.530	*	0.794	0.616	†	0.755	0.667	†
Avg	0.649	0.506	*	0.855	0.829	*	0.927	0.875	*

	GCIPL	**mRNFL**	**SRC-VD**	***P* Value**	**GCIPL**	**mRNFL**	**SRC-VD**	***P* Value**	**GCIPL**	**mRNFL**	**SRC-VD**	***P* Value**
ST	0.619	0.596	0.541	*	0.773	0.674	0.545	†	0.880	0.755	0.576	‡
Sup	0.695	0.564	0.519	*	0.796	0.651	0.523	†	0.882	0.705	0.559	‡
SN	0.690	0.515	0.657	*	0.717	0.703	0.476	‡	0.800	0.706	0.623	†
IN	0.628	0.521	0.643	*	0.855	0.811	0.454	‡	0.872	0.828	0.591	‡
Inf	0.598	0.561	0.623	*	0.975	0.888	0.433	‡	0.968	0.914	0.544	‡
IT	0.589	0.579	0.599	*	0.964	0.889	0.500	‡	0.975	0.923	0.614	‡
Avg	0.687	0.554	0.634	*	0.918	0.829	0.559	‡	0.946	0.866	0.705	‡

Sup, superior; Nas, nasal; Inf, inferior; Temp, temporal.
* $P \geq 0.05$.
† $P < 0.05$.
‡ $P \leq 0.01$.

(i.e., RPC and SRC) since glaucoma is a disease of the RGCs and their axons (i.e., RNFs),[1] which are nourished by those plexuses; moreover, deep capillary plexus may be affected by projection artifacts.[31] The radial capillary plexus has peculiar features that distinguish it from other retinal capillary plexuses.[32–34] Firstly described more than 50 years ago in histologic specimens, RPCs originate from precapillary arterioles at the posterior pole and are intimately associated with RNFs, which are mostly nourished by this specific plexus.[34] Since they parallel RNFs, RPCs are mainly located in the infero- and superotemporal peripapillary areas, are less prominent in the infero- and superonasal sectors, and are absent in the foveal and perifoveal regions.[34] Beyond their location, RPCs have other distinguishing features; specifically, they proceed on longer and straighter paths and have few anastomoses to each other.[34] Experimental studies conducted on animal models illustrated that RPCs are more vulnerable to IOP elevation, suggesting that underfilling of such capillaries could play a primary role.[32] In modern times, OCT-A was able to isolate the RPC plexus by setting the segmentation slab between ILM and RNFL/ganglion cell layer interface, and it confirmed in vivo most of the previous observations.[33] In our study, we specifically looked at RPC-VD in the peripapillary retina and found that glaucomatous eyes exhibited a marked reduction on average and in all quadrants except for the nasal one compared to GS and controls. The present finding is in accordance with previous studies, using different instruments, algorithms, and postprocessing techniques.[4–6,8,35–37] With regard to the correlation analysis between structural and vascular variables, we found a significant association between pRNFL and RPC-VD, especially in the G group, who exhibited a significant correlation also between RPC-VD and functional damage. This is in accordance with the observations by Yu and colleagues,[38] who demonstrated ex vivo that RPC volume and RNFL thickness are closely correlated. Notably, we appreciated significant differences between GS and controls for structural parameters but not for vascular parameters at the peripapillary area. In this regard, one may hypothesize that this structural/microvascular mismatch indicates that neurodegeneration occurs prior to vascular damage, and therefore capillary dropouts may be secondary to loss of RNFs. Another explanation is that OCT-A could not be as sensitive as structural OCT to detect early changes and thus could miss subtle vascular capillary rarefaction. Further studies with longitudinal rather than cross-sectional design are warranted to answer this question.

In addition to RPC-VD, we also focused differences of SRC-VD in the macula across the three groups. Differently from RPCs, SRCs have a centripetal pattern with many interconnections to each other (forming a honeycomb pattern) and to more superficial and deeper vascular plexuses.[33] SRCs feed and match the RGCs and therefore they interrupt in correspondence of the foveola forming a capillary-free zone, named foveal avascular zone.[39] In our study, we did not find any significant difference regarding SRC-VD across the three groups, either average or sectorial. Moreover, we explored correlations across structural, vascular, and functional parameters also for the macular area. In this regard, we have applied vascular analysis of the same grid (i.e., GCIPL grid) used for the GCIPL thickness structural analysis. Notably, this is the first report showing the vessel perfusion density calculated after superimposing the GCIPL grid on OCT-A images, allowing an accurate correlation between the two compartments (i.e., structure, microvasculature). However, SRC-VD did not correlate with structural variables (i.e., GCIPL thickness, mRNFL thickness) or VF MD. Once again, the discrepancy between structural and microvascular damage could indicate a primary neurodegeneration, followed by capillary dropouts. The same considerations as discussed above may apply. In this regard, however, Shoji and colleagues[12] observed in a longitudinal study progressive decrease in macular vessel perfusion density of glaucomatous eyes with no evidence of change in GCC thickness. Our results in the macular area differ from those reported by previous studies, where glaucomatous eyes exhibited a significant reduction of macular VD.[10,11,13,15] Several considerations must be made to explain our finding. First, methodological differences across studies must be acknowledged, since the OCT-A device used,[40,41] angiocube sizes (i.e., 3×3, 4.5×4.5, 6×6 mm),[42] the vessel perfusion density calculation algorithm, ROI, and image quality[43] may have a significant impact. Furthermore, the SRC segmentation used by most OCT-A devices, including the one used in the present study, include not only the superficial capillary plexus, but also part of the intermediate plexus, which is not involved in glaucomatous disease, as well as the deep capillary plexus, as shown using a projection-resolved algorithm by Takusagawa et al.[13] In addition, we observed that some capillary dropout areas following an arcuate path resembling the RNFL topography run peripheral to our ROI, and therefore they could be at least in part missed by our OCT-A analysis. As experimentally demonstrated by Alterman and Henkind,[32] RPCs are the most damaged in the situation of glaucomatous damage, and thus macular capillaries of the SRC could be relatively spared from glaucomatous damage.

From a diagnostic point of view, all structural parameters performed better than the vascular ones. Despite being inferior to structural parameters, the diagnostic ability of RPC-VD was still good; conversely, SRC-VD analysis led to poor performance and therefore is not useful for glaucoma diagnosis. Our results are in perfect agreement with those illustrated by Rao and colleagues.[11] Conversely, Chen et al.[10] found that SRC-VD had excellent diagnostic accuracy comparable to structural variables. Discordance among studies could be related to differences in the study population (e.g., glaucoma severity) or study design, or related to OCT-A technical aspects discussed above.

The main limitation of our study is related to the relatively small sample size. In addition, we did not measure axial length in our cohort of patients, and therefore magnification related to axial length differences could have biased our study with regard to the quantification of structural and vascular parameters.[44–46] In the attempt to limit such artifacts, we excluded eyes with significant refractive errors.

Despite those limitations, several conclusions can be drawn from the present study. First, structural damage is evident both in the peripapillary (i.e., GS and glaucoma) and in the macular (i.e., glaucoma) areas. Vascular damage seems to be less prominent, as it was seen only for the G group and only at the RPC. The structural/vascular mismatch could be explained by primary neurodegenerative mechanism and secondary involvement of retinal vasculature; higher vulnerability of RPCs; and less sensitivity of OCT-A compared to structural OCT to identify early changes. Finally, diagnostic abilities are excellent for structural variables, less so but still good for RPC-VD, and poor for SRC-VD.

Acknowledgments

Disclosure: **G. Triolo**, None; **A. Rabiolo**, None; **N.D. Shemonski**, Carl Zeiss Meditec, Inc. (E); **A. Fard**, Carl Zeiss Meditec, Inc. (E); **F. Di Matteo**, None; **R. Sacconi**, None; **P. Bettin**, None; **S. Magazzeni**, Carl Zeiss Meditec, Inc. (E); **G. Querques**, Alimera Sciences (C), Allergan, Inc. (C), Bayer Schering-Pharma (C), Heidelberg (C), Novartis (C), Sandoz (C), Zeiss (C); **L.E. Vazquez**, None; **P. Barboni**, None; **F. Bandello**, Allergan (S), Alimera (S), Bayer (S), Farmila-Thea (S), Schering Pharma (S), Sanofi-Aventis (S),

Novagali (S), Pharma (S), Hoffmann-La Roche (S), Genentech (S), Novartis (S)

References

1. Weinreb RN, Leung CK, Crowston JG, et al. Primary open-angle glaucoma. *Nat Rev Dis Primers*. 2016;2:16067.
2. Hood DC, Slobodnick A, Raza AS, de Moraes CG, Teng CC, Ritch R. Early glaucoma involves both deep local, and shallow widespread, retinal nerve fiber damage of the macular region. *Invest Ophthalmol Vis Sci*. 2014;55:632–649.
3. Rabiolo A, Carnevali A, Bandello F, Querques G. Optical coherence tomography angiography: evolution or revolution? *Expert Rev Ophthalmol*. 2016;11:243–245.
4. Lee EJ, Lee KM, Lee SH, Kim TW. OCT Angiography of the peripapillary retina in primary open-angle glaucoma. *Invest Ophthalmol Vis Sci*. 2016;57:6265–6270.
5. Mammo Z, Heisler M, Balaratnasingam C, et al. Quantitative optical coherence tomography angiography of radial peripapillary capillaries in glaucoma, glaucoma suspect, and normal eyes. *Am J Ophthalmol*. 2016;170:41–49.
6. Mansoori T, Sivaswamy J, Gamalapati JS, Balakrishna N. Radial peripapillary capillary density measurement using optical coherence tomography angiography in early glaucoma. *J Glaucoma*. 2017;26:438–443.
7. Shin JW, Lee J, Kwon J, Choi J, Kook MS. Regional vascular density-visual field sensitivity relationship in glaucoma according to disease severity [published online ahead of print April 21, 2017]. *Br J Ophthalmol*. doi:10.1136/bjophthalmol-2017-310180.
8. Yarmohammadi A, Zangwill LM, Diniz-Filho A, et al. Optical coherence tomography angiography vessel density in healthy, glaucoma suspect, and glaucoma eyes. *Invest Ophthalmol Vis Sci*. 2016;57:OCT451–OCT459.
9. Yarmohammadi A, Zangwill LM, Diniz-Filho A, et al. Relationship between optical coherence tomography angiography vessel density and severity of visual field loss in glaucoma. *Ophthalmology*. 2016;123:2498–2508.
10. Chen HS, Liu CH, Wu WC, Tseng HJ, Lee YS. Optical coherence tomography angiography of the superficial microvasculature in the macular and peripapillary areas in glaucomatous and healthy eyes. *Invest Ophthalmol Vis Sci*. 2017;58:3637–3645.
11. Rao HL, Pradhan ZS, Weinreb RN, et al. A comparison of the diagnostic ability of vessel density and structural measurements of optical coherence tomography in primary open angle glaucoma. *PLoS One*. 2017;12:e0173930.
12. Shoji T, Zangwill LM, Akagi T, et al. Progressive macula vessel density loss in primary open angle glaucoma: a longitudinal study. *Am J Ophthalmol*. 2017;182:107–117.
13. Takusagawa HL, Liu L, Ma KN, et al. Projection-resolved optical coherence tomography angiography of macular retinal circulation in glaucoma. *Ophthalmology*. 2017;124:1589–1599.
14. Xu H, Yu J, Kong X, Sun X, Jiang C. Macular microvasculature alterations in patients with primary open-angle glaucoma: a cross-sectional study. *Medicine (Baltimore)*. 2016;95:e4341.
15. Yarmohammadi A, Zangwill LM, Diniz-Filho A, et al. Peripapillary and macular vessel density in patients with glaucoma and single-hemifield visual field defect. *Ophthalmology*. 2017;124:709–719.
16. Kotowski J, Folio LS, Wollstein G, et al. Glaucoma discrimination of segmented cirrus spectral domain optical coherence tomography (SD-OCT) macular scans. *Br J Ophthalmol*. 2012;96:1420–1425.
17. Mwanza JC, Oakley JD, Budenz DL, Chang RT, Knight OJ, Feuer WJ. Macular ganglion cell-inner plexiform layer: automated detection and thickness reproducibility with spectral domain-optical coherence tomography in glaucoma. *Invest Ophthalmol Vis Sci*. 2011;52:8323–8329.
18. Banitt MR, Ventura LM, Feuer WJ, et al. Progressive loss of retinal ganglion cell function precedes structural loss by several years in glaucoma suspects. *Invest Ophthalmol Vis Sci*. 2013;54:2346–2352.
19. Lalezary M, Medeiros FA, Weinreb RN, et al. Baseline optical coherence tomography predicts the development of glaucomatous change in glaucoma suspects. *Am J Ophthalmol*. 2006;142:576–582.
20. Miki A, Medeiros FA, Weinreb RN, et al. Rates of retinal nerve fiber layer thinning in glaucoma suspect eyes. *Ophthalmology*. 2014;121:1350–1358.
21. Kiddee W, Tantisarasart T, Wangsupadilok B. Performance of optical coherence tomography for distinguishing between normal eyes, glaucoma suspect and glaucomatous eyes. *J Med Assoc Thai*. 2013;96:689–695.
22. Oli A, Joshi D. Can ganglion cell complex assessment on cirrus HD OCT aid in detection of early glaucoma? *Saudi J Ophthalmol*. 2015;29:201–204.
23. Flammer J, Mozaffarieh M. What is the present pathogenetic concept of glaucomatous optic neuropathy? *Surv Ophthalmol*. 2007;52(suppl 2):S162–S173.
24. Raitta C, Sarmela T. Fluorescein angiography of the optic disc and the peripapillary area in chronic glaucoma. *Acta Ophthalmol (Copenh)*. 1970;48:303–308.
25. Yokoyama Y, Aizawa N, Chiba N, et al. Significant correlations between optic nerve head microcirculation and visual field defects and nerve fiber layer loss in glaucoma patients with myopic glaucomatous disk. *Clin Ophthalmol*. 2011;5:1721–1727.
26. Marjanovic I, Milic N, Martinez A, Benitez-del-Castillo J. Retrobulbar hemodynamic parameters in open-angle and angle-closure glaucoma patients. *Eye (Lond)*. 2012;26:523–528.
27. Wang Y, Fawzi AA, Varma R, et al. Pilot study of optical coherence tomography measurement of retinal blood flow in retinal and optic nerve diseases. *Invest Ophthalmol Vis Sci*. 2011;52:840–845.
28. Logan JF, Rankin SJ, Jackson AJ. Retinal blood flow measurements and neuroretinal rim damage in glaucoma. *Br J Ophthalmol*. 2004;88:1049–1054.
29. Burgansky-Eliash Z, Bartov E, Barak A, Grinvald A, Gaton D. Blood-flow velocity in glaucoma patients measured with the retinal function imager. *Curr Eye Res*. 2016;41:965–970.
30. Schuman JS. Measuring blood flow: so what? *JAMA Ophthalmol*. 2015;133:1052–1053.
31. Spaide RF, Fujimoto JG, Waheed NK. Image artifacts in optical coherence tomography angiography. *Retina*. 2015;35:2163–2180.
32. Alterman M, Henkind P. Radial peripapillary capillaries of the retina. II. Possible role in Bjerrum scotoma. *Br J Ophthalmol*. 1968;52:26–31.
33. Campbell JP, Zhang M, Hwang TS, et al. Detailed vascular anatomy of the human retina by projection-resolved optical coherence tomography angiography. *Sci Rep*. 2017;7:42201.
34. Henkind P. Radial peripapillary capillaries of the retina. I. Anatomy: human and comparative. *Br J Ophthalmol*. 1967;51:115–123.
35. Akil H, Huang AS, Francis BA, Sadda SR, Chopra V. Retinal vessel density from optical coherence tomography angiography to differentiate early glaucoma, pre-perimetric glaucoma and normal eyes. *PLoS One*. 2017;12:e0170476.
36. Liu L, Jia Y, Takusagawa HL, et al. Optical coherence tomography angiography of the peripapillary retina in glaucoma. *JAMA Ophthalmol*. 2015;133:1045–1052.

Investigative Ophthalmology & Visual Science

37. Scripsema NK, Garcia PM, Bavier RD, et al. Optical coherence tomography angiography analysis of perfused peripapillary capillaries in primary open-angle glaucoma and normal-tension glaucoma. *Invest Ophthalmol Vis Sci*. 2016;57:OCT611–OCT620.
38. Yu PK, Cringle SJ, Yu DY. Correlation between the radial peripapillary capillaries and the retinal nerve fibre layer in the normal human retina. *Exp Eye Res*. 2014;129:83–92.
39. Cicinelli MV, Carnevali A, Rabiolo A, et al. Clinical spectrum of macular-foveal capillaries evaluated with optical coherence tomography angiography. *Retina*. 2017;37:436–443.
40. Munk MR, Giannakaki-Zimmermann H, Berger L, et al. OCT-angiography: a qualitative and quantitative comparison of 4 OCT-A devices. *PLoS One*. 2017;12:e0177059.
41. De Vitis LA, Benatti L, Tomasso L, et al. Comparison of the performance of two different spectral-domain optical coherence tomography angiography devices in clinical practice. *Ophthalmic Res*. 2016;56:155–162.
42. Dong J, Jia YD, Wu Q, et al. Interchangeability and reliability of macular perfusion parameter measurements using optical coherence tomography angiography [published online ahead of print March 23, 2017]. *Br J Ophthalmol*. doi:10.1136/bjophthalmol-2016-309441.
43. Al-Sheikh M, Falavarjani KG, Akil H, Sadda SR. Impact of image quality on OCT angiography based quantitative measurements. *Int J Retina Vitreous*. 2017;3:13.
44. Sampson DM, Gong P, An D, et al. Axial length variation impacts on superficial retinal vessel density and foveal avascular zone area measurements using optical coherence tomography angiography. *Invest Ophthalmol Vis Sci*. 2017;58:3065–3072.
45. Kang SH, Hong SW, Im SK, Lee SH, Ahn MD. Effect of myopia on the thickness of the retinal nerve fiber layer measured by Cirrus HD optical coherence tomography. *Invest Ophthalmol Vis Sci*. 2010;51:4075–4083.
46. Nakanishi H, Akagi T, Hangai M, et al. Effect of axial length on macular ganglion cell complex thickness and on early glaucoma diagnosis by spectral-domain optical coherence tomography. *J Glaucoma*. 2016;25:e481–e490.

Investigative Ophthalmology & Visual Science